Temperature-gradient–induced instability in polymer films

EUROPHYSICS LETTERS 15 October 2002

Europhys. Lett., **60** (2), pp. 255–261 (2002)

Temperature-gradient–induced instability in polymer films

E. SCHÄFFER[1](*), S. HARKEMA[1], R. BLOSSEY[2] and U. STEINER[1](**)

[1] *Department of Polymer Chemistry and Materials Science Center University of Groningen - Nijenborgh 4, NL-9747 AG Groningen, The Netherlands*

[2] *Zentrum für Bioinformatik, Universität des Saarlandes D-66123 Saarbrücken, Germany*

(received 6 June 2002; accepted in final form 5 August 2002)

PACS. 68.15.+e – Liquid thin films.
PACS. 68.60.-p – Physical properties of thin films, nonelectronic.
PACS. 82.35.Lr – Physical properties of polymers.

Abstract. – We report the experimental observation and a theoretical model for a thin-film instability caused by a temperature gradient. A polymer-air double layer sandwiched between two plates set to different temperatures shows an instability leading to polymer columns or stripes spanning the two plates. The characteristic wavelength of these patterns scales inversely with the initial heat flux through the double layer. Theoretically, we describe the heat flow in terms of the diffusion of heat through the bilayer, causing an interfacial radiation pressure that destabilizes the film.

Surface instabilities of liquids have intrigued scientists for more than a century [1] and continue to be the subject of intensive research. Apart from the technological importance of thin films, this is mainly due to the fact that the break-up of thin films sensitively mirrors the minute forces that act at the film's interface. The most extensively studied example of the effect of interfacial forces on film stability is the dewetting of thin supported polymer films [2,3]. Here, film instabilities occur either spontaneously, driven by van der Waals forces [4], or are nucleated [5]. In addition, film break-up caused by electrostatic [6–8] and elastic forces [9] has also been reported.

The signature of spontaneous film instabilities (as opposed to heterogeneously nucleated instabilities) is the emergence of a characteristic undulation, which leads to the film break-up. The well-defined wavelength of this surface wave is a result of the force balance at the film surface (*i.e.* the destabilizing force *vs.* surface tension that tends to minimize the surface area). Consequently, a film in the absence of a destabilizing force is stable with respect to the thermal fluctuations of its interface. Quantitatively, such film instabilities are well described by a linear stability analysis [2, 10], which calculates the hydrodynamic response of the film to a perturbation of its interfacial position. Here, we discuss a new interfacial instability caused by a laterally homogeneous temperature gradient that is applied perpendicular to a polymer-air double layer.

(*) Present address: Max Planck Institute of Molecular Cell Biology and Genetics - 01307 Dresden, Germany.
(**) E-mail: u.steiner@chem.rug.nl

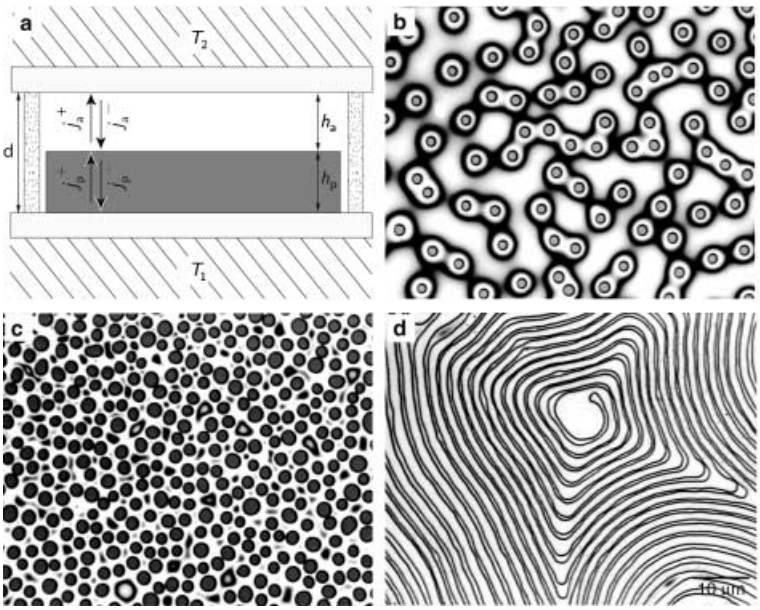

Fig. 1 – (a) Schematic cross-section of the experimental set-up. A liquid PS film is destabilized by a heat flux across the film, which is the consequence of the applied temperature difference between the top and bottom plate. Silicon oxide spacers maintain a constant range of plate spacings d in a wedge geometry (*e.g.*, d varies slightly from left to right). (b)-(d) Optical micrographs of polystyrene films which were heated in the set-up shown in (a). Columnar and striped patterns were observed, often on the same sample. The formation of columnar patterns are shown in (b) (early stage) and (c) (late stage), corresponding to different locations on the same sample with $h = 100\,\mathrm{nm}$ and $\Delta T = 46\,^\circ\mathrm{C}$ (in (b): $d = 345\,\mathrm{nm}$, in (c): $d = 285\,\mathrm{nm}$). The striped pattern in (d) typically showed a linear or spiral morphology ($h = 110\,\mathrm{nm}$, $d = 170\,\mathrm{nm}$, $\Delta T = 54\,^\circ\mathrm{C}$).

The experimental set-up is shown in fig. 1a. A thin polystyrene (PS; molecular weight: 108 kg/mol) film of thickness h_p was spin-coated onto a highly polished silicon wafer [11]. Facing the PS film, a second silicon wafer was mounted. The distance between the plates d was kept constant by silicon oxide spacers which were sputtered onto the top wafer (dotted areas). This assembly was placed onto a hotplate set to the temperature $T_1 = 170\,^\circ\mathrm{C}$. As a heat sink, a water-cooled copper block maintained at a temperature T_2 was put onto the top plate, establishing the temperature difference $\Delta T = T_1 - T_2$ across the film and the air gap. Both temperatures were above the glass transition temperature of PS and were kept constant with a precision of $\pm 1\,^\circ\mathrm{C}$. Typically, the polymer films were $h_\mathrm{p} \approx 100\,\mathrm{nm}$ thick and the plate spacings d ranged from 120 nm to 600 nm. For values of ΔT of 10–55 °C, this resulted in high-temperature gradients of $\sim 10^8\,^\circ\mathrm{C\,m^{-1}}$. After annealing overnight, the sample was quenched to room temperature and the top plate was removed. To prevent the adhesion of polymer to the top plate, the silicon wafer was rendered non-polar by deposition of a self-assembled alkane monolayer. A range of d values could be obtained in a single experiment by using a wedge geometry of the assembly (*i.e.* by varying d by $\approx 1\,\mu\mathrm{m}$ over a lateral distance of 1 cm). The topography of the vitrified polymer films was investigated after removal of the top plate using optical and atomic-force microscopy (AFM).

Using the sample set-up in fig. 1a, two different film morphologies were observed as shown in fig. 1b-d. The film instability resulted either in polymer columns spanning the two plates (early stage: fig. 1b, late stage: fig. 1c) or in a stripe pattern (fig. 1d). We concentrate here on

the origins of the instability. The difference in morphologies will be discussed elsewhere [12]. For a given set of parameters (h, d, ΔT —see fig. 1a), the column diameter ($1.9 \pm 0.2\,\mu$m) in fig. 1b was well defined, while the columns themselves were stochastically distributed with an inter-column spacing $\lambda = 2.9 \pm 0.6\,\mu$m (fig. 1c). The morphology of the columns gives qualitative information about the break-up of the film. The well-defined column diameter in fig. 1b shows that the instability which led to the column formation occurred at a well-defined time. The stochastic column distribution indicates the absence of inter-column interactions. The polymer morphologies in fig. 1b-d are a direct consequence of the applied temperature gradient. Control experiments, in which the set-up in fig. 1a was annealed in an oven ($\Delta T = 0$), showed no such instabilities.

A quantitative analysis of images similar to those in fig. 1b-d is shown in fig. 2a. The characteristic spacing λ was obtained by directly measuring the distance between columns and stripes, in regions of homogeneously distributed lateral structures. Within the limits of the scatter of the data, λ scales linearly with d. In addition, λ is a decreasing function of the applied temperature difference ΔT. An experiment was also performed with a polymer film that was deposited onto a gold surface (100 nm Au on a silicon wafer —squares in fig. 2a). Surprisingly, the choice of substrate has a strong effect on the wavelength of the instability. For otherwise similar experimental parameters, λ is lowered by a factor of ≈ 4, compared to films that were directly spin-coated onto silicon wafers.

The morphology in fig. 1b, c is reminiscent of a spontaneous (spinodal) film instability, comparable, for example, to the dewetting of thin films [3,5] or electrohydrodynamic structure formation [7,8]. While seemingly similar, the cause of the instability is fundamentally different. Usually, dewetting is described as the transition from an unstable (or metastable) toward a stable state. Since such instabilities develop slowly, the system is quasi-static and the free energy of the system can be defined at any time. In our case, the film-air double layer has to be described by non-equilibrium thermodynamics. In particular, there is no equivalent of a Gibbs' free energy [13].

To gain an understanding of the origins of the instability, we have developed a scaling argument that accounts for the instability. Before embarking on the derivation of a model, it is important to identify the mechanism of heat conduction in the film. In macroscopic liquids heat transport occurs predominantly by convection, giving rise to the well-understood convective in-

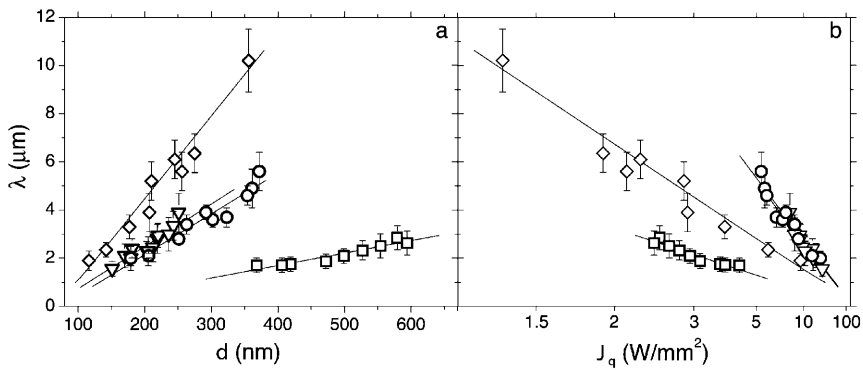

Fig. 2 – Plot of the experimentally determined instability wavelength λ *vs.* the plate spacing d (a) and the heat flux J_q (b). The diamonds, triangles and circles correspond to polystyrene films with $h = 96$ nm, $\Delta T = 11\,^\circ$C, $h = 80$ nm, $\Delta T = 43\,^\circ$C and $h = 100$ nm, $\Delta T = 46\,^\circ$C, respectively. The squares represent a 92 nm thick polystyrene film which was spin-coated onto a gold (100 nm) covered silicon substrate ($\Delta T = 37\,^\circ$C).

stabilities. In very thin, highly viscous films, however, Rayleigh-Bénard or Marangoni-Bénard convection are suppressed. The onset of convection is determined by the critical values of the dimensionless Rayleigh (R) and Marangoni (M) numbers [14]. For our experimental parameters, R and M of the polymer film were lower by 16 and 8 orders of magnitude, respectively, compared to their critical values for convection. Also in the air gap, R and M were much below their critical values. The transfer of heat across the double layer takes place by heat diffusion exclusively. In the polymer film, heat transport occurs by the diffusion of local (segmental) molecular motion. In the air gap, thermal transport occurs by the translational diffusion of gas molecules.

For diffusive thermal motion, the heat flux is given by Fourier's law

$$J_q = -\kappa \frac{\partial T}{\partial z} \tag{1}$$

with the thermal conductivity κ. For the double-layer system in fig. 1a, the temperature profile from T_1 to T_2 consists of a shallow gradient in the polymer (κ_p) and a steep gradient in the air layer (κ_a). J_q within each layer is given by the linear equation $J_q = \kappa_i \Delta T_i / h_i$, with κ_i the heat conductivity, ΔT_i the temperature variation across the layer i, and h_i the film thickness. The thermal conductivities of the two plates are much larger than κ_p and κ_a, so that the plates are isothermal. Since the overall heat flow is the same as the flux through the individual layers,

$$J_q = \frac{\kappa_\mathrm{a}\kappa_\mathrm{p}\Delta T}{\kappa_\mathrm{a} h_\mathrm{p} + \kappa_\mathrm{p} h_\mathrm{a}} \,. \tag{2}$$

In the absence of convection, molecular vibrations in the liquid transport the heat. As postulated by Debye [15] thermal excitations are high-frequency wave packets, comparable to phonons in crystalline solids. In this model, the flux of thermal energy J_q causes a momentum flux [16] in the direction of lower temperatures [17]

$$J_\mathrm{p} = \frac{J_q}{u} \tag{3}$$

with the velocity of sound u. Acoustic radiation impinging on an interface between two semi-infinite media with the reflectivity R causes a radiation pressure

$$p = -\frac{2RJ_q}{u} \,. \tag{4}$$

In the bilayer system of fig. 1a, the partial energy fluxes in each layer (j_p^+, j_p^-, j_a^+, j_a^-) and the fluxes that are coupled in and out of the heat source and sink (j_1^+, j_1^-, j_2^+, j_2^-) have to be considered. The 8 flux components are coupled by the reflectivities and transmissions R_{ik} and $\mathcal{T}_{ik} = 1 - R_{ik}$

$$j_i^- = \mathcal{T}_{i+1,i} j_{i+1}^- + R_{i,i+1} j_i^+ \,, \tag{5a}$$

$$j_i^+ = \mathcal{T}_{i-1,i} j_{i-1}^+ + R_{i,i-1} j_i^- \tag{5b}$$

with the indices i, k, referring to the two layers (p, a) and the two plates $(1, 2)$ [18]. The net heat flux is given by

$$J_q = j_\mathrm{p}^+ - j_\mathrm{p}^- = j_\mathrm{a}^+ - j_\mathrm{a}^- \tag{6}$$

and the pressure acting at the polymer surface is

$$p = \frac{1}{u_\mathrm{a}}(j_\mathrm{a}^+ + j_\mathrm{a}^-) - \frac{1}{u_\mathrm{p}}(j_\mathrm{p}^+ + j_\mathrm{p}^-) \tag{7}$$

with u_a, u_p the velocities of sound in the air and the polymer, respectively.

For our experimental conditions, we have $j_\mathrm{a}^- \ll J_q$ (see below) and we can set $j_2^- \approx 0$ and $j_2^+ \approx J_q$. Using these boundary conditions, eqs. (5) can be iteratively solved. The resulting equations depend on the interfacial reflectivities and are linear in J_q. Since R_{ik} is not J_q-dependent, eq. (4) is replaced by the scaling equation

$$p = -\frac{2\bar{Q}}{u_\mathrm{p}} J_q \,. \tag{8}$$

$\bar{Q}(R_{ik}, u_i)$ is a measure of the acoustic quality of the polymer film. Positive values of the quality factor $\bar{Q}$ lead to a destabilization of the polymer film, as calculated by a linear stability analysis [2, 10]. For a polymer-air interface with a surface tension γ, the most unstable wavelength of a surface undulation is

$$\lambda = 2\pi \left(-\frac{1}{2\gamma} \frac{\partial p}{\partial h_2} \right)^{-\frac{1}{2}} . \tag{9}$$

Since the disjoining pressure is negligible, eqs. (8) and (2) give

$$\lambda = 2\pi \sqrt{\frac{\gamma u_\mathrm{p} \Delta T}{\bar{Q}} \frac{\kappa_\mathrm{p}\kappa_\mathrm{a}}{(\kappa_\mathrm{p} - \kappa_\mathrm{a})}} \frac{1}{J_q} \,. \tag{10}$$

To test the prediction of eq. (10), we have plotted the experimentally determined values of λ *vs.* J_q in fig. 2b. Our data confirms the scaling equation (10) in two ways. It not only mirrors the reciprocal scaling of λ with J_q, we also find a unique value for $\bar{Q}$ for a given experimental system. For the Si-PS-air-Si sandwich, we find $\bar{Q} = 6.2$ and for the Au-PS-air-silicon we have $\bar{Q} = 83$. This is reasonable, since $\bar{Q}$ is a function of R_{ik} and u_i only and should not depend on the geometric parameters, or the temperature difference.

The quantitative prediction of the $\bar{Q}$-factor requires a detailed description of the heat diffusion through both layers and their coupling at all three interfaces. As opposed to simple liquids, the high-frequency rheological behavior of polymers is glassy even at temperatures above their glass transition temperature (at 0 Hz). This implies that acoustic waves up to several 100 GHz have a relatively large mean-free-path length ($\sim 1\,\mu$m) [19, 20]. They propagate acoustically and reflect specularly off interfaces. Close to the Debye limit ($\nu_\mathrm{D} \sim 1$ THz), phonon propagation in any material is diffusive (*i.e.* their mean-free-path length is small (~ 1 Å)). In addition, interfaces are rough on the length scale of the acoustic wavelength. Therefore, the interfacial coupling of the heat flux is diffusive. The two boundary conditions lead to a mode-dependent interfacial reflectivity: $R_{ik}^\mathrm{l} = [(Z_i - Z_k)/(Z_i + Z_k)]^2$ and $R_{ik}^\mathrm{h} = (u_k^2)/(u_i^2 + u_k^2)$, where the indices l, h refer to low- and high-frequency modes, respectively. $Z_i = \rho_i u_i$ is the acoustic impedance of medium i with the density ρ_i [21].

While the scaling description remains in essence correct, eqs. (5) have to be understood in terms of the partial flux per mode (with an energy of $k_\mathrm{B}T$ each). The total flux J_q (eq. (6)) and the total interfacial pressure (eq. (7)) have to be obtained by integration over the Debye density of states ($J_q = C \int_0^{\nu_\mathrm{D}} j_q \nu^2 \mathrm{d}\nu$). In the absence of more detailed information, we model the mode-dependent R_{ik} as a step function with a cross-over frequency ν_c,

$$J_q = C \left[\int_0^{\nu_\mathrm{c}} \hat{\mathcal{T}}_\mathrm{l} j_1^+ \nu^2 \mathrm{d}\nu + \int_{\nu_\mathrm{c}}^{\nu_\mathrm{D}} \hat{\mathcal{T}}_\mathrm{h} j_1^+ \nu^2 \mathrm{d}\nu \right] , \tag{11}$$

$$p = -\frac{2C}{u_\mathrm{p}} \left[\int_0^{\nu_\mathrm{c}} Q_\mathrm{l} \hat{\mathcal{T}}_\mathrm{l} j_1^+ \nu^2 \mathrm{d}\nu + \int_{\nu_\mathrm{c}}^{\nu_\mathrm{D}} Q_\mathrm{h} \hat{\mathcal{T}}_\mathrm{l} j_1^+ \nu^2 \mathrm{d}\nu \right] . \tag{12}$$

$\hat{T}$ is the overall heat transmission through the bilayer per mode $j_q = \hat{T} j_1^+$ (as obtained from eqs. (5)) and C is a constant. By comparison of eqs. (2) and (11), and eqs. (4) and (12), it is possible to derive $\bar{Q}$ in a self-consistent fashion. In the limit where $\hat{T}_\mathrm{l} \ll \hat{T}_\mathrm{h}$, we have

$$\bar{Q} \approx f \frac{\hat{T}_\mathrm{l}}{\hat{T}_\mathrm{h}} Q_\mathrm{l} + Q_\mathrm{h}\,, \tag{13}$$

with $f = 1/[(\nu_\mathrm{D}/\nu_\mathrm{c})^3 - 1]$.

While the detailed derivation of $\bar{Q}$ will be published elsewhere [12], we discuss here qualitatively some of its essential parts. First, it is important to note that heat transport at the polymer-air interface is not symmetrical ($R_\mathrm{pa} \neq R_\mathrm{ap}$) due to the differences in the heat transport in the polymer and air layers. Air molecules approaching the interface are temporarily adsorbed at the interface, thereby equilibrating to the interfacial temperature [22]. The effective interfacial heat transfer implies that $R_\mathrm{ap} = R_\mathrm{a2} \approx 0$ and therefore $j_\mathrm{a}^- \approx 0$. Using eqs. (5), (7), and (8), $\bar{Q}$ is defined in terms of R_{ik}. In the low-frequency limit, the acoustic reflection of thermal vibrations implies $R_\mathrm{pa}^\mathrm{l} \approx 1$ and we have $Q_\mathrm{l} \approx 1/(1 - R_\mathrm{pa})$, while close to the Debye limit $R_\mathrm{pa} \approx 0$ and $Q_\mathrm{h} \approx -(u_\mathrm{p}/u_\mathrm{a} - 1)/2$.

Qualitatively, $R_\mathrm{pa}^\mathrm{l} \approx 1$ and $Q_\mathrm{l} = +\mathrm{O}(1000)$ means that low-frequency modes conduct only little of the heat, but cause a substantial destabilizing interfacial pressure. At high frequencies, on the other hand, we have $R_\mathrm{pa}^\mathrm{h} \approx 0$ and $Q_\mathrm{h} = -\mathrm{O}(1)$, leading to an effective heat transport across the double layer causing only a small (stabilizing) interfacial pressure. The only unknown parameter in eq. (13) is the cross-over frequency ν_c. For the experimentally determined value of $\bar{Q} = 6.7$, we find from eq. (13) $\nu_\mathrm{c} \approx 0.96\nu_\mathrm{D}$. The value of $\nu_\mathrm{c} = \mathrm{O}(\nu_\mathrm{D})$ is not unreasonable, confirmed by measurements that show that longitudinal acoustic waves propagate acoustically up to several THz [19]. In spite of the high value of ν_c, more than 90% of the heat is transported by the high-frequency modes [23].

In summary, 1) we have found experimentally that a thin polymer film becomes unstable when confined between two plates set to different temperatures. The observed instability shows a preferentially amplified mode and is therefore reminiscent of a spinodal instability; 2) assuming an interfacial radiation pressure that is caused by the heat flux, we have developed a scaling argument that predicts a reciprocal dependence of the instability wavelength on the heat flux, a dependence that is borne out by our data; 3) we have formulated a model that is based on the microscopic mechanism of heat diffusion [12]. In this model, we divide the thermal flux into two parts. Low-frequency waves propagate acoustically and are nearly perfectly reflected off the polymer-air interface. They cause a destabilizing radiation pressure but conduct only little heat. High-frequency modes propagate diffusively. With only little interfacial resistance (and therefore only a small interfacial pressure), they are essential to establish the steady-state heat flux across the bilayer.

* * *

We thank T. Thurn-Albrecht for stimulating discussions and acknowledge financial support by the "Stichting voor Fundamenteel Onderzoek der Materie" (FOM) and by the Deutsche Forschungs Gemeinschaft (DFG) (SFB513, priority program "Wetting and structure formation at surfaces").

REFERENCES

[1] Rayleigh L., *Proc. London Math. Soc.*, **10** (1878) 4.
[2] Brochard-Wyart F. and Daillant J., *Can. J. Phys.*, **68** (1990) 1084.

[3] Reiter G., *Phys. Rev. Lett.*, **68** (1992) 75.
[4] Seemann R., Herminghaus S. and Jacobs K., *J. Phys. Condens. Matter*, **13** (2001) 4925.
[5] Jacobs K., Mecke K. and Herminghaus S., *Langmuir*, **14** (1998) 965.
[6] Herminghaus S., *Phys. Rev. Lett.*, **83** (1999) 2359.
[7] Schäffer E., Thurn-Albrecht T., Russell T. P. and Steiner U., *Nature*, **403** (2000) 874.
[8] Schäffer E., Thurn-Albrecht T., Russell T. P. and Steiner U., *Europhys. Lett.*, **53** (2001) 518.
[9] Mönch W. and Herminghaus S., *Europhys. Lett.*, **52** (2001) 525.
[10] Vrij A., *J. Colloid Sci.*, **19** (1964) 1.
[11] As received, the silicon wafers were covered by a native oxide layer. They were cleaned in a jet of CO_2 ice crystals ("snow-jet": Sherman R., Hirt D. and Vane R., *J. Vac. Sci. Technol.*, **12** (1876) 1994).
[12] Schäffer E., Roerdink M., Harkema S., Blossey R. and Steiner U., submitted to *Macromolecules*.
[13] Schmittmann B. and Zia R. K. P., *Phase Transitions and Critical Phenomena*, Vol. **17** (Academic Press, London) 1995.
[14] Cross M. C. and Hohenberg P. C., *Rev. Mod. Phys.*, **65** (1993) 851.
[15] Debye P., *Ann. Phys.*, **39** (1912) 789.
[16] Since the propagation of a longitudinal wave does not result in the net displacement of the liquid, J_q is the pseudo-momentum flux of the waves (the distinction between momentum and pseudo-momentum is necessary whenever a medium is involved). The pseudo-momentum is, however, subject to a similar conservation law as the true momentum. Consequently, conservation of pseudo-momentum can be used to compute real forces. For the boundary condition in our experiment, the conservation of pseudo-momentum results in the Rayleigh radiation pressure in eq. (4) (see Stone M., arXiv:cond-mat (2000), `http://arXiv.org/abs/cond-mat/0012316`).
[17] Albanese C., Dell'Aversana P. and Gaeta F. S., *Phys. Rev. Lett.*, **79** (1997) 4151.
[18] The numbering sequence in eq. (5) is 1, p, a, 2.
[19] Sette F., Krisch M. H., Masciovecchio C., Ruocco G. and Monaco G., *Science*, **280** (1998) 1550.
[20] Morath C. J. and Maris H. J., *Phys. Rev. B*, **54** (1996) 203.
[21] Swartz E. T. and Pohl R. O., *Rev. Mod. Phys.*, **61** (1989) 605.
[22] Knudsen M., *Ann. Phys. (Leipzig)*, **34** (1911) 593.
[23] The much higher $\bar{Q}$-factor for the Au-covered substrate stems from differences on how the heat is coupled in at the substrate interface. This will be discussed elsewhere [12].